On the Energy Distribution of Fast Atoms Emerging from Tokamak Plasmas

H.M. Mayer

IPP III/28 August 1976

MAX-PLANCK-INSTITUT FÜR PLASMAPHYSIK

8046 GARCHING BEI MÜNCHEN

MAX-PLANCK-INSTITUT FÜR PLASMAPHYSIK

GARCHING BEI MÜNCHEN

On the Energy Distribution of Fast Atoms Emerging from Tokamak Plasmas

H.M. Mayer

IPP III/28 August 1976

Die nachstehende Arbeit wurde im Rahmen des Vertrages zwischen dem Max-Planck-Institut für Plasmaphysik und der Europäischen Atomgemeinschaft über die Zusammenarbeit auf dem Gebiete der Plasmaphysik durchgeführt.

IPP III/28

On the Energy Distribution of Fast Atoms Emerging from Tokamak Plasmas

H.M.Mayer

August 1976

Abstract

Assuming rotational symmetry and a local Maxwellian (and thereby neglecting particle drifts) energy spectra have been calculated for i) asymptotic conditions $E/T_o \gg 1, E/T_o \ll 1$ (T_o = peak ion temperature) ii) model profiles for plasma density and temperature as well as neutral atom concentration. For plasmas extending several mean free paths in radius an energy is estimated around which T_o may be preferably obtained as the inverse logarithmic derivative of the flux sepctrum.

The results indicate that collection of a significant number of particles in the Maxwellian tail ($E \gtrsim 8\ T_o$) should allow a fairly accurate determination of T_o even if the hot region is separated from the outside by many mean free paths.

Introduction

In the research directed towards thermonuclear fusion the diagnosis of the spatial and temporal behaviour of the ion temperature is one of the fundamental tasks. Considering in particular Tokamaks, the most powerful method used at present is the analysis of the small sample of ions which succeed in escaping from the magnetic trap via the process

$$H^+(\underline{v}_1) + H^\circ(\underline{v}_2) \rightarrow H^\circ(\underline{v}_1) + H^+(\underline{v}_2)$$

in which an electron changes its nucleonic partner. With increasing size and plasma density in present-day Tokamaks this method becomes limited by the burn-out of the neutral target as well as by reabsorption of the neutralized ions on their way towards the plasma surface. Therefore, without further analysis, one may be sceptical about obtaining information from the plasma center whenever the plasma radius is considerably larger than the attenuation length and at the same time the density of neutrals has decayed by several orders of magnitude from the plasma edge to the hot core.

The situation, however, may be not quite as hopeless as it looks at the first glance provided that the distribution of the ions is Maxwellian (or that deviations are calculable and do not lead to severe distortion of the high energy tail).

In contrast to previous studies of this topic based on the Boltzmann equation /1/ /2/ which suffered from the neglect of the temperature profiles the following analysis is purely phenomenological and ignores almost completely the physical origin of the profiles discussed. In this respect it resembles the treatment of a selected case given in /3/. However, by establishing explicitly the asymptotic shape of the energy spectrum and by treating a variety of model profiles its main purpose is to remove some of the uncertainty so far

encountered in the interpretation of experimental data obtained from dense plasmas /4/.

Energy distribution at origin

Introducing

$E(x)$ for the energy of hydrogen ions (or atoms)

$n(x)$ for the density of hydrogens ions (assuming $n_i = n_e$)

$H(x)$ for the density of hydrogens atoms

$T(x)$ for the ion temperature (assuming $T_e = T_i$)

$\sigma(E)$ for the cross-section for charge transfer

$\langle \sigma v \rangle$ for the charge exchange rate averaged over the distribution of relative velocities $v_{oi} \equiv |v_o - v|$, $m_H v^2/2 = E$

$\langle \sigma v \rangle_I$ for the ionization rate averaged over the distribution of relative velocities $v_{oe} \equiv |v_o - v_e|$, $m_e v_e^2/2 = T_e/3$

We can write the number of neutrals produced per second in $d^3x\, dE$ as

$$d^4 J_o = \frac{2}{\sqrt{\pi}} \left(\frac{E}{T}\right)^{1/2} \frac{dE}{T} e^{-E/T} n \langle \sigma v \rangle H\, d^3x \qquad (1)$$

Absorption

On their way to the plasma surface these fast neutrals will be attenuated (primarily by charge exchange but also by ionization processes). Introducing an effective cross-section for attenuation by

$$\sigma_A = (n\lambda)^{-1} = (\langle \sigma v \rangle + \langle \sigma v \rangle_I)/v_o \,, \qquad (2)$$

we can define an attenuation factor

$$A(r,a) \equiv e^{s(r)-\rho} \quad ; \quad s(r) \equiv \int_0^r dr'/\lambda \, , \; s(a) \equiv \rho(E) \qquad (3)$$

in which s measures the particles distance from r = o in units of its mean free path. We call $\rho \equiv s(a)$ the "absorption radius" of the discharge.

Approximation: The following "cold target"-approximation will become convenient

$$E \gg T : \qquad \langle \sigma v \rangle \approx \sigma v_r$$
$$s \approx \sigma_A \int_0^r n \, dr' \qquad (4)$$

The "temperature" of the neutral gas must be considerably below T over large regions of the discharge. For this reason the error introduced by the above approximation will remain modest even where the condition $E \gg T$ is violated. We shall accept it troughout in this paper.

Energy distribution of emerging atoms

We assume a local Maxwellian and evaluate the flux of hydrogen atoms which leaves the plasma from a surface element dO into a narrow cone $d\Omega$ around the diameter by summing up all the attenuated contributions (1):

$$d^3\Phi = \frac{d\Omega}{4\pi} \, dO \, dJ_o$$

where

$$dJ_o = e^{-\rho} \int_{-a}^{a} A(r,o) \, H \langle \sigma v \rangle n \cdot \frac{2}{\sqrt{\pi}} \left(\frac{E}{T}\right)^{1/2} e^{-E/T} \frac{dE}{T} \, dr \, . \qquad (5)$$

From now on we are going to study the result of the integration (5) under special conditions.

Analytic treatment of limiting cases

Next we want to consider cases in which the integral of eq.(5) can be carried out analytically. Apart from the trivial case of an isothermal plasma, expansions can be made for low and for high energies which lead to elementary integrals.

a) $T(r) = T(0) = T_o$ (isothermal plasma): From eqs.(3) and (5)

$$dJ_o = \langle\sigma v\rangle \frac{2}{\sqrt{\pi}} \left(\frac{E}{T_o}\right)^{1/2} e^{-E/T_o} \frac{dE}{T_o} e^{-\rho \int_{-a}^{a} A_+ H n \, dr} \qquad (6)$$

Here the attenuation has been split into a part referring to $r = o$ and an odd and an even remainder:

$$A(r,a) = e^{-\rho}(A_- + A_+) \; ; \; A_- = Sh\, s \, , \; A_+ = Ch\, s \qquad (7)$$

of which only the latter contributes to the integral.

b) $E \gg T_o$ (asymptotic behaviour at high energies): We note that the integrand of eq.(5) becomes more and more peaked around $r = o$ when E increases towards large values. An expansion of the type

$$e^{-E/T} A_+ H n T^{-3/2} = H_o n_o T_o^{-3/2-\varepsilon} e \cdot e^{\left(h^{-2} + \lambda^{-2} + d^{-2} - \frac{3}{2} t^{-2} + \varepsilon t^{-2}\right) \frac{r^2}{2} + \cdots} \qquad (8)$$

where

$$\varepsilon \equiv E/T_o \; ; \; h^{-2} \equiv \left.\frac{H''}{H}\right|_{r=o} ; \; d^{-2} \equiv \left.\frac{n''}{n}\right|_{r=o} ; \; t^{-2} \equiv \left.\frac{T''}{T}\right|_{r=o}$$

allows analytical integration between limits $r = \pm\infty$ yielding ($\varepsilon \gg 1$)

$$\frac{dJ_o}{d\varepsilon} = 2^{3/2} |t| H_o n_o \langle\sigma v\rangle \left(\frac{\varepsilon}{\varepsilon - \varepsilon_1}\right)^{1/2} e^{-\rho - \varepsilon} \; ; \; \varepsilon_1 \equiv \frac{3}{2} - \frac{t^2}{h^2} - \frac{t^2}{\lambda^2} - \frac{t^2}{d^2} \qquad (9)$$

where the energy dependence is described by the last four factors. For non-inverted temperature profiles

t^2 is negative by defintion, hence ε_1 can become considerably larger than unity.

We can use eq.(9) for a qualitative discussion of the high energy tail of the flux spectrum. The factor $\exp(-\rho)$ has the effect of a "high pass filter" which attenuates the high energy tail of the spectrum less heavily than the lower energies, whereas the factor in front of it has the opposite effect of enhancing the energies close to $E_1 = \varepsilon_1 T_o$ at which the approximation breaks down. Between the two regions an energy usually exists at which the logarithmic plot of the flux spectrum has just the "right" slope which corresponds to the exponent $-E/T_o$. Making use of eqs.(3), (4) and (9) this energy is given by

$$\varepsilon^* = \varepsilon_1 \left(\frac{1}{.7\rho(E^*) + .5} + 1 \right) \overset{\rho \gg 1}{\sim} \varepsilon_1 \qquad (10)$$

(In (10) we have used the power laws $\sigma_A \propto E^{-0.35}$ $\langle \sigma v \rangle \propto E^{0.25}$ as an approximation for energies relevant to Tokamak experiments).

An alternative expression for the high energy tail of the spectrum is obtained by the use of

$$\frac{H}{H_o} = \mathrm{Ch}\,\frac{r}{h} \qquad (11)$$

as an approximate description of the atomic profile in the central region of the discharge. The choice (11) can be motivated to some extent by the similarity of the absorption for the bulk of incoming atoms with the absorption of outgoing atoms of energy E as described by eqs.(3) and (7). In place of Eq.(9) we obtain

$$\frac{dJ_o}{d\varepsilon} = 2^{3/2} |t| H_o n_o \langle \sigma v \rangle \left(\frac{\varepsilon}{\varepsilon - \varepsilon_2} \right)^{1/2} \frac{e^{\frac{x_+^2/2}{\varepsilon - \varepsilon_2}} + e^{\frac{x_-^2/2}{\varepsilon - \varepsilon_2}}}{2} e^{-\rho - \varepsilon} \qquad (12)$$

where

$$\varepsilon_2 = \frac{3}{2} - \frac{t^2}{d^2} \; , \quad \varkappa_\pm = \frac{|t|}{h} \pm \frac{|t|}{\lambda}$$

The break-down of the approximation is now shifted towards the lower energy $\varepsilon_2 T_o$. The advantage over eq.(9) is relativated, however, to some extent because the region of validity is approached less rapidly by eq.(12) (Fig.1).

c) $E \sim T_a \ll T_o$ (asymptotic behaviour at low energies)
No experimental evidence seems to exist so far for this case due to the difficulties to detect and analyze neutral atoms at energies below 150 eV. We nevertheless want to derive approximate expressions for this part of the spectrum as well.

Due to the fact that the neutral gas concentration decreases steeply at the plasma edge, contributions to the low energy end of the spectrum come almost entirely from the vicinity of the plasma surface. The expansion

$$A\,H\langle\sigma v\rangle n T^{-3/2} = H_a \langle\sigma v\rangle n_a T_a^{-3/2} e^{-\frac{E}{T_a}} e^{\left(\gamma^{-1} + \frac{E}{T_a}\tau^{-1}\right)\xi + \cdots} \tag{13}$$

where

$$\xi \equiv (r-a) \; ; \quad \tau^{-1} = \frac{T'}{T}\Big|_{r=a} \; ; \quad \gamma^{-1} \equiv \left[-\lambda^{-1} + \frac{(Hn\langle\sigma v\rangle)'}{Hn\langle\sigma v\rangle} - \frac{3}{2}\frac{T'}{T}\right]_{r=a} < 0$$

may be integrated between the limits $\xi = 0$ and $\xi = \infty$ (instead of $\xi = o$ and $\xi = 2a$) as long as $-\left(\gamma^{-1} + \frac{E}{T_a}\tau^{-1}\right) \gg a^{-1}$ yielding

$$dJ_o = H_a n_a \langle\sigma v\rangle \frac{2}{\sqrt{\pi}} \left(\frac{E}{T_a}\right)^{1/2} \frac{dE}{T_a} \frac{e^{-E/T_a}}{\left|\gamma^{-1} + \frac{E}{T_a}\tau^{-1}\right|} \; ; \; \frac{E}{T_a} \ll \frac{\tau}{|\gamma|} \tag{14}$$

Eq.(14) predicts a maximum which is located at

$$\begin{aligned} E_{max} &\sim T_a \quad \text{for} \quad \tau \gg 4|\gamma| \\ E_{max} &\lesssim 2T_a \quad \text{for} \quad \tau \gtrsim 4|\gamma| \end{aligned} \tag{15}$$

From eqs. (14) and (15) we conclude that the position and the absolute value of the maximum will be determined mainly by the ion temperature and the concentration of hydrogen atoms close to the plasma surface - which is exactly what we expected.

The asymptotic spectra of equs.(9),(12) and (14) are shown in Fig.1.

Calculations made with model profiles

Eqs.(13) and (16) demonstrate that at energies somewhat above $\varepsilon_1 T_o$ the shape of the spectrum becomes independent of the details of the profiles and - except from $\langle\sigma v\rangle$ - is influenced only by the energy dependence of $\rho(E)$. The easiest way to determine the peak ion temperature would then be to make use of this simple asymptotic behaviour. In practice, however, one has to struggle against the exponential decrease of counting rates which often have the tendency to become burried in background noise (for example due to γ-radiation). For plasmas for which $a/\lambda_o \gg 1$ this makes it necessary to use a part of the spectrum which is still influenced by the plasma and neutral gas profiles in the vicinity of the axis.

In order to estimate roughly the magnitude of corrections necessary to compensate this influence we have computed flux spectra using profiles of the following kind:

$$n(x) = n_o \cos^{\nu} \frac{\pi}{2} \frac{x}{a} \qquad \nu = 0,\ 1$$

$$T(x) = T_o \cos^{\vartheta} \frac{\pi}{2} \frac{x}{a} \qquad \vartheta = 1.0,\ 1.5,\ 2.0 \qquad (16)$$

$$H(x) = H_o \mathrm{Ch} \frac{x}{h} \qquad \lambda_o \equiv \lambda(T_o) = 0.7\ h$$

The decay length h of the atomic profile has been coupled to the mean free path for atoms of energy $E = T_o$ and chosen to be roughly $\sqrt{2}\,\lambda_o$. The choice of a coupling factor

close to this value was advocated by numerical results obtained with the Düchs code /5/ as well as by a more detailed consideration of the atomic diffusion /6/.[+)]

It is evident that the quantities λ_o and h cannot be independent since λ_o characterizes the attenuation of outgoing atoms of energy T_o whereas h plays a similar role for the bulk of incoming atoms of somewhat lower energy. The latter circumstance could suggest to take $h < \lambda_o$, in contrast to the choice made above. On the other hand "diffusive" charge transfer collisions dominate over "absorbing" ionizing collisions and lead to representative ratios $\lambda_o/h \lesssim 1$. Yet we cannot deny that there remains some degree of arbitrariness in the fixation $\lambda_o = 0.7\ h$ which therefore should be replaced by a more detailed analysis /6/ for quantitative applications.

Of course, the simple expression used for the atomic profile can only describe the central region in a satisfactory manner. On the other hand we may neglect the distant regions as long as we only want to describe the high energy tail of the spectrum correctly.

The cross-sections used in the numerical calculations are

$$\sigma/cm^2 = 2\cdot 10^{-15}\,(E/kev)^{-1/4} \qquad (17)$$
$$\sigma_A/cm^2 = 2\cdot 10^{-15}\left[(E/kev)^{-1/4} + .36\,(E/kev)^{-1/2}\right]$$

The second term in σ_A which describes ionization is about 50 % higher than the value for ionization from ground state with $T_e = T_i = T$. We justify this enhancement by the fact that in an actual Tokamak plasma ionization tends to be increased by i) the possibility of ionization from exited states ii) the possibility of $T_e > T_i$ iii) the presence of impurities which make $n_e > n_i \equiv n$.

[+)] To demonstrate the dependence on the coupling factor. Tables 1a and 2a have been calculated for $h = \lambda_o$

Results obtained from calculations with model profiles are shown in Figs.2 and 3. They illustrate the effect of increasing absorption radius and of the influence of the parameters ϑ, γ and T_o on the spectrum. In Fig.4 comparison was made with a Düchs code simulation /4/ /5/ of a PULSATOR discharge with pulsed gas inflow (crosses). The agreement is good. From inspection of these figures one also concludes that whenever $\varepsilon_1 >> 1$ is satisfied, this quantity can replace ε^*, serving as a useful criterion for the energy at which T_o may be obtained from the logarithmic plot of the neutral flux spectrum.

From Tables 1 and 2 the deviations of the flux spectrum from a simple exponential law are obtained in the form of the quantities

$$Q \equiv e^{E/T_o} dJ_o/d(E/T_o) <\sigma v>_o H_o n_o a d0 \qquad (18)$$

and

$$R \equiv T_o/T_\phi - 1 \quad \text{with} \quad T_\phi^{-1} \equiv E_n^{-1} \ln \frac{J_o(E_n)}{J_o(2E_n)} \qquad (19)$$

where the latter is the correction that would have to be applied in order to obtain the value of T_o from the portion of the flux curve which lies between E_n and $2E_n$. Table 3 gives a summary over all the expressions used in this paper to describe the flux spectrum. Table 4 has been extracted from Table 2 after rescaling to the "slope temperature".

Conclusions

From the results obtained we conclude that as long as there are no serious distortions of the Maxwellian distribution, and the density and temperature profiles are conventional determinations of the peak ion temperature should be possible even if several attenuation lengths have to be traversed. It is then necessary to collect as many energetic atoms as possible by maximizing the acceptance and the (stripping-) efficiency of the analyzer. If pulsed gas admission is used during the discharge the plane of observation should be close

to the orifice. Serious distortions of the Maxwellian arise from high frequency or injection heating; distortions can also be caused by trapped particle drifts /7/.

For dense and/or large plasmas for which $a/\lambda_o \gtrsim 3$ it is recommended to consider the asymptotic form of the spectrum rather than the isothermal approximation in order to derive the peak ion temperature.

Acknowledgements

The author wishes to thank M.Walter for carrying out the numerical integrations, D.F.Düchs, F.Wagner and S.Rehker for discussions. It is to D.F.Düchs that he owes the opportunity to use results of his computer simulations. Thanks are also due to H.Volkenandt and S.Zettl for help in preparing the manuscript.

References

/1/ O.V.Konstantinov and V.I.Perel, Sov.Phys.Tech.Phys.5, 1403 (1961)

/2/ S.Rehker and H.Wobig, Plasma Physics 15, 1083 (1973)

/3/ C.R.Parsons and S.S.Medley, Plasma Physcs 16, 267 (1974)

/4/ A.I.Kislyakov et al., IPP III/25(1976), laboratory report

/5/ D.F.Düchs, Proc.Vth Europ.Conf.on Contr.Fusion and Plasma Physics, Grenoble 1972, Vol.I, p.14.
see also reference /4/

/6/ H.M.Mayer, to be published

/7/ M.P.Petrov, Sov.Phys.Tech.Phys.13, 708 (1968)

Figures

Fig. 1: Asymptotic behaviour and model calculations of the flux sepctrum

Fig. 2: Model spectra for various values of a/λ_o
Density profile: $\cos \frac{\pi}{2} \frac{r}{a}$
Temperatures profiles: $\cos \frac{\pi}{2} \frac{r}{a}$ and $\cos^2 \frac{\pi}{2} \frac{r}{a}$

Fig. 3: Model spectra for various values of γ and T_o
$a/\lambda_o = 4$. Temperature profiles: $\cos^{1,5} \frac{\pi}{2} \frac{r}{a}$

Fig. 4: Comparison of model spectra with a Düchs code simulation of a high density PULSATOR discharge

Tables

Table 1 $Q \equiv e^{E/T_o} \cdot dJ_o/d(\frac{E}{T_o}) \langle \sigma v \rangle_o H_o n_o$ adO for $\bar{h}^{-1} = .7\, \lambda_o^{-1}$ and various values of a/λ_o, ϑ, γ and T_o

Table 2 Relative correction necessary to apply if T_o is derived from the logarithmic slope of the flux spectrum between energies E_n and $2\,E_n$

Tables 1a, 2a as Tables 1 and 2, however choosing $\bar{h}^{-1} = \lambda_o^{-1}$

Table 3 Summary of expressions used to describe the energy spectrum of the atomic flux.

Table 4 $F \equiv T_o/T_{\phi n}$; $T_{\phi n} \equiv E_n^{-1} \ln \frac{J_o(E_n)}{J_o(2E_n)}$
= correction factor after rescaling to the "slope temperature" between energies E_n and $2\,E_n$

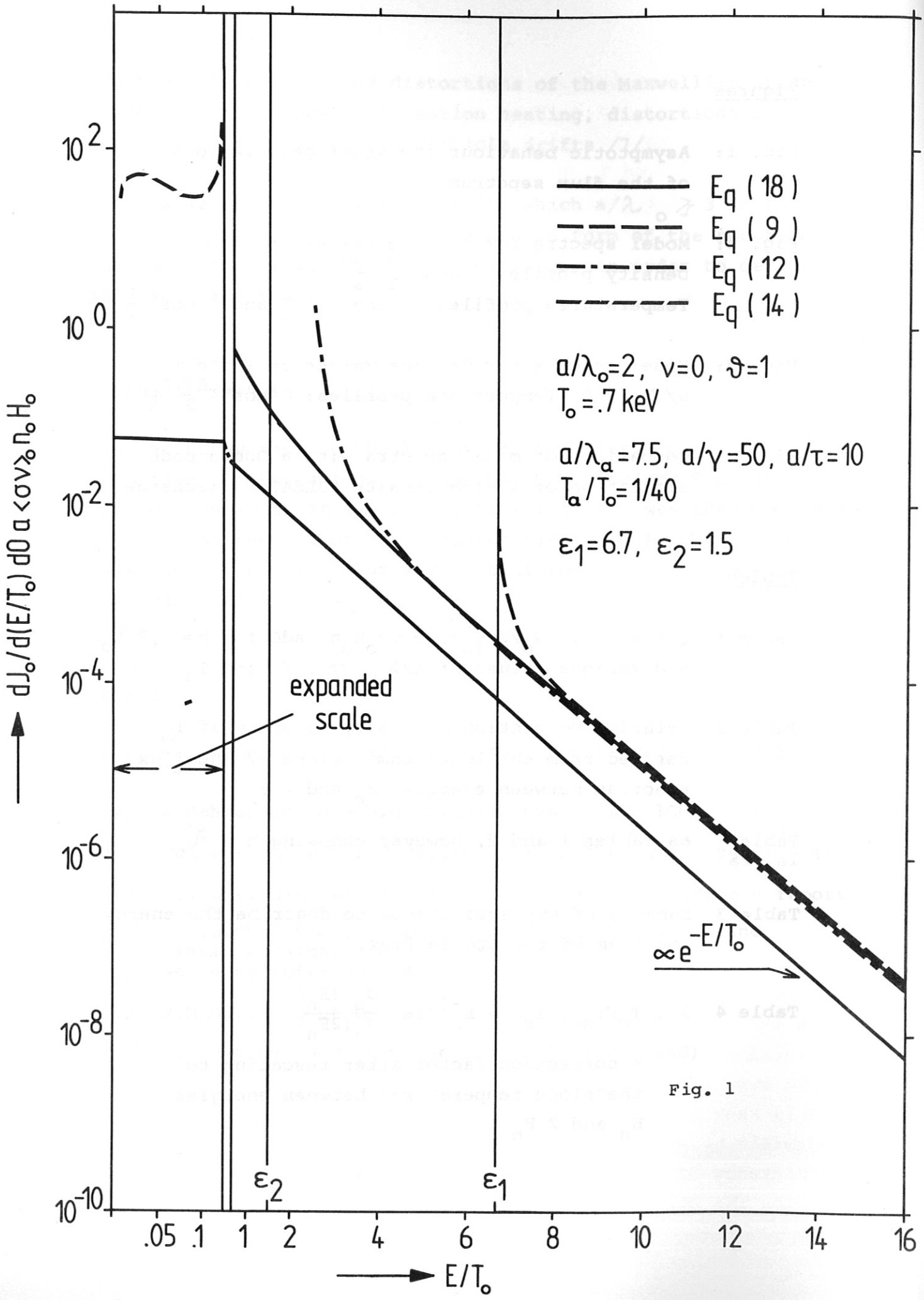
10^2
10^0
10^{-2}
10^{-4}
10^{-6}
10^{-8}
10^{-10}
$dJ_o/d(E/T_o)\, d\Omega\, a\langle\sigma v\rangle_o n_o H_o$
Eq (18)
Eq (9)
Eq (12)
Eq (14)
$a/\lambda_o=2$, $\nu=0$, $\vartheta=1$
$T_o=.7$ keV
$a/\lambda_\alpha=7.5$, $a/\gamma=50$, $a/\tau=10$
$T_\alpha/T_o=1/40$
$\varepsilon_1=6.7$, $\varepsilon_2=1.5$
expanded scale
$\propto e^{-E/T_o}$
ε_2
ε_1
.05 .1 1 2 4 6 8 10 12 14 16
E/T_o

Fig. 1

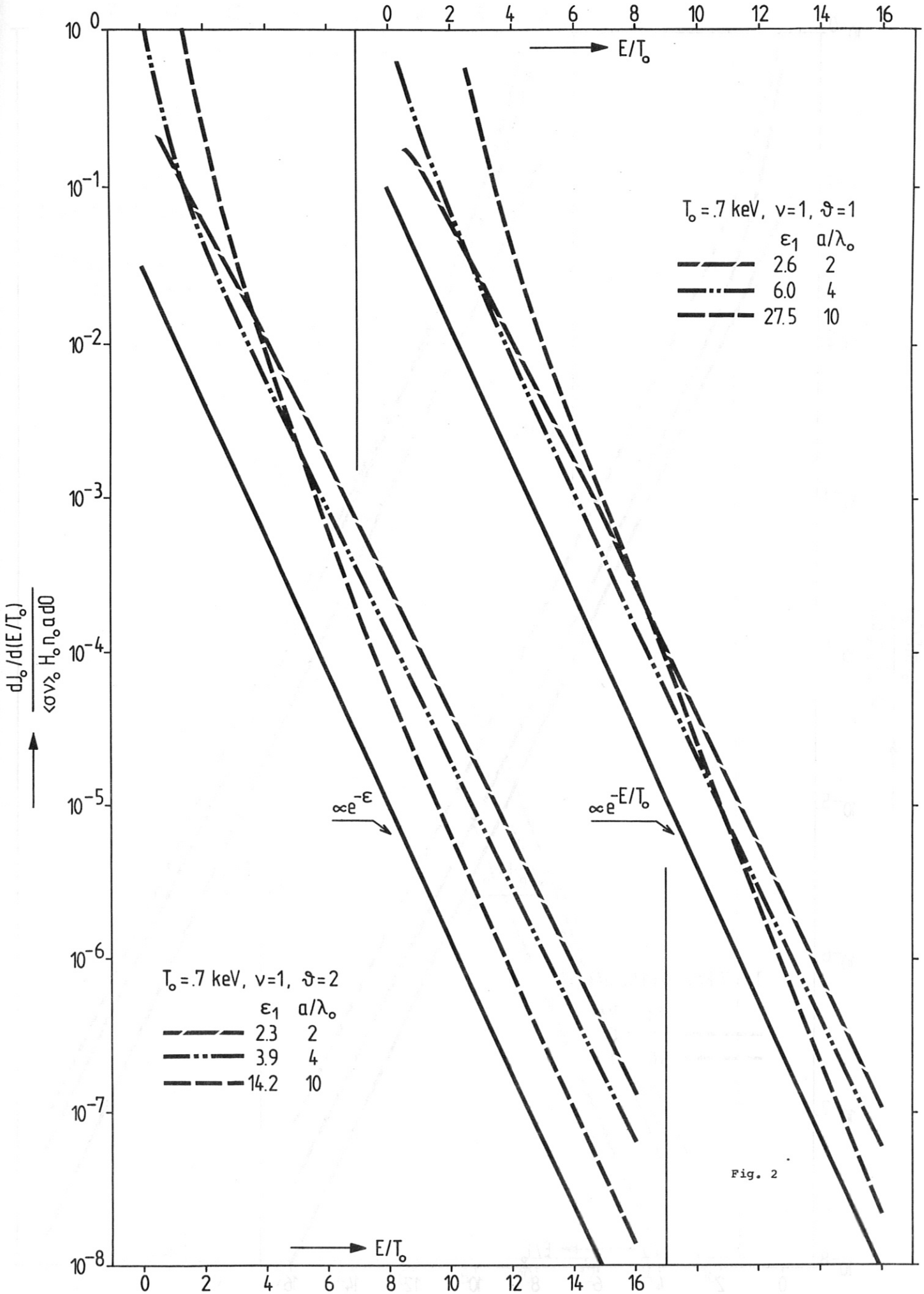
T_o = .7 keV, ν=1, ϑ=1
ε_1 a/λ_o
2.6 2
6.0 4
27.5 10
T_o = .7 keV, ν=1, ϑ=2
ε_1 a/λ_o
2.3 2
3.9 4
14.2 10
$\propto e^{-\varepsilon}$
$\propto e^{-E/T_o}$
E/T_o
E/T_o
$\frac{dJ_o/d(E/T_o)}{\langle\sigma v\rangle_o H_o n_o a d\Omega}$

Fig. 2

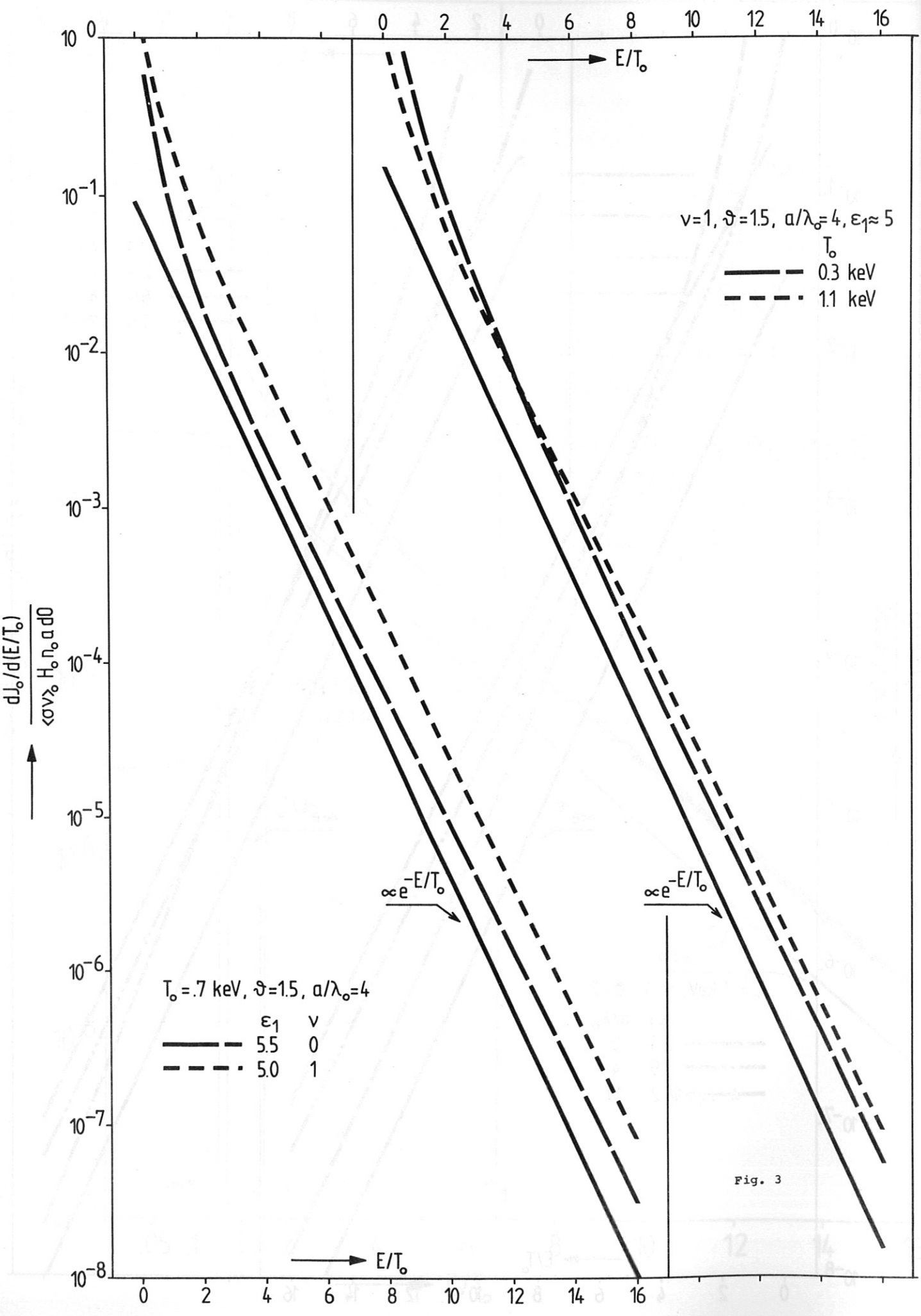
$\frac{dJ_o/d(E/T_o)}{\langle\sigma v\rangle_o H_o n_o a\, d\Omega}$
10^{0}
10^{-1}
10^{-2}
10^{-3}
10^{-4}
10^{-5}
10^{-6}
10^{-7}
10^{-8}
0 2 4 6 8 10 12 14 16
E/T_o
$\nu=1$, $\vartheta=1.5$, $a/\lambda_o=4$, $\varepsilon_1\approx 5$
T_o
0.3 keV
1.1 keV
$\propto e^{-E/T_o}$
$\propto e^{-E/T_o}$
$T_o=.7$ keV, $\vartheta=1.5$, $a/\lambda_o=4$
ε_1 ν
5.5 0
5.0 1
E/T_o

Fig. 3

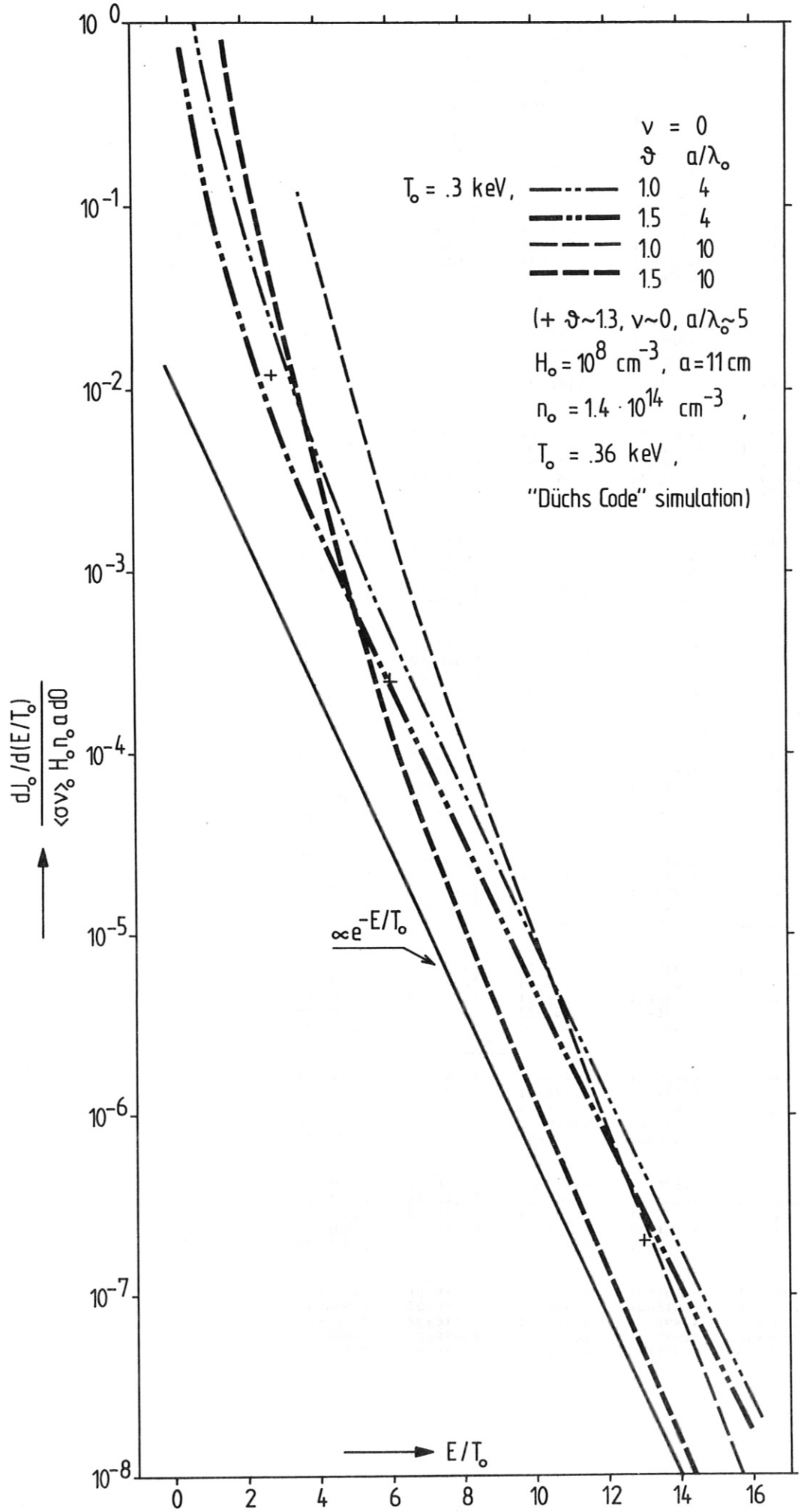
10^0
10^{-1}
10^{-2}
10^{-3}
10^{-4}
10^{-5}
10^{-6}
10^{-7}
10^{-8}
0
2
4
6
8
10
12
14
16
$\frac{dJ_o/d(E/T_o)}{\langle\sigma v\rangle_o H_o n_o a d0}$
E/T_o
$\propto e^{-E/T_o}$
T_o = .3 keV,
ν = 0
ϑ a/λ$_o$
1.0 4
1.5 4
1.0 10
1.5 10
(+ ϑ~1.3, ν~0, a/λ$_o$~5
$H_o = 10^8$ cm^{-3}, a=11 cm
$n_o = 1.4 \cdot 10^{14}$ cm^{-3},
T_o = .36 keV,
"Düchs Code" simulation)

Fig. 4

T_o keV	ϑ	E_n/T_o	a/λ_o = 1.	2.	4.	10.	20.
		1.0	5.19E-01	4.61E-01	1.29E+00	1.92E+02	5.18E+06
		2.0	6.33E-01	3.76E-01	5.59E-01	2.78E+01	2.15E+05
	1.0	4.0	8.45E-01	3.93E-01	2.69E-01	3.10E+00	4.46E+03
		8.0	1.17E+00	5.22E-01	1.91E-01	3.51E-01	5.56E+01
		16.0	1.62E+00	7.73E-01	2.26E-01	6.48E-02	6.94E-01
		1.0	3.91E-01	2.46E-01	3.60E-01	1.01E+01	2.41E+04
		2.0	4.91E-01	2.21E-01	1.69E-01	1.46E+00	8.52E+02
.3	1.5	4.0	6.73E-01	2.67E-01	1.02E-01	2.02E-01	1.97E+01
		8.0	9.44E-01	3.91E-01	1.00E-01	3.62E-02	3.95E-01
		16.0	1.31E+00	6.07E-01	1.52E-01	1.32E-02	1.22E-02
		1.0	3.18E-01	1.55E-01	1.35E-01	9.18E-01	2.49E+02
		2.0	4.12E-01	1.56E-01	7.33E-02	1.65E-01	1.13E+01
	2.0	4.0	5.74E-01	2.09E-01	5.55E-02	3.14E-02	3.95E-01
		8.0	8.12E-01	3.24E-01	6.91E-02	8.74E-03	1.47E-02
		16.0	1.13E+00	5.15E-01	1.19E-01	5.31E-03	1.03E-03
		1.0	6.27E-01	4.38E-01	7.13E-01	2.15E+01	3.20E+04
		2.0	7.98E-01	4.36E-01	3.95E-01	4.48E+00	2.23E+03
	1.0	4.0	1.06E+00	5.28E-01	2.65E-01	8.13E-01	9.37E+01
		8.0	1.43E+00	7.31E-01	2.64E-01	1.71E-01	2.99E+00
		16.0	1.92E+00	1.06E+00	3.67E-01	6.41E-02	1.22E-01
		1.0	5.05E-01	2.78E-01	2.69E-01	2.14E+00	4.57E+02
		2.0	6.44E-01	2.98E-01	1.62E-01	4.61E-01	2.92E+01
.7	1.5	4.0	8.63E-01	3.93E-01	1.35E-01	1.04E-01	1.43E+00
		8.0	1.17E+00	5.72E-01	1.70E-01	3.33E-02	7.38E-02
		16.0	1.57E+00	8.47E-01	2.70E-01	2.24E-02	6.85E-03
		1.0	4.28E-01	2.00E-01	1.28E-01	3.42E-01	1.32E+01
		2.0	5.52E-01	2.32E-01	8.90E-02	8.81E-02	1.06E+00
	2.0	4.0	7.44E-01	3.23E-01	8.94E-02	2.62E-02	7.52E-02
		8.0	1.01E+00	4.84E-01	1.30E-01	1.23E-02	6.65E-03
		16.0	1.36E+00	7.26E-01	2.22E-01	1.25E-02	1.23E-03
		1.0	6.96E-01	4.52E-01	5.80E-01	9.05E+00	4.08E+03
		2.0	8.92E-01	4.88E-01	3.64E-01	2.24E+00	3.63E+02
	1.0	4.0	1.18E+00	6.17E-01	2.87E-01	5.11E-01	2.13E+01
		8.0	1.57E+00	8.56E-01	3.23E-01	1.43E-01	1.05E+00
		16.0	2.07E+00	1.22E+00	4.65E-01	7.38E-02	7.29E-02
		1.0	5.72E-01	3.08E-01	2.50E-01	1.20E+00	9.57E+01
		2.0	7.30E-01	3.53E-01	1.72E-01	3.08E-01	8.03E+00
1.1	1.5	4.0	9.64E-01	4.73E-01	1.65E-01	8.70E-02	5.59E-01
		8.0	1.28E+00	6.79E-01	2.22E-01	3.66E-02	4.42E-02
		16.0	1.69E+00	9.82E-01	3.52E-01	3.19E-02	6.66E-03
		1.0	4.93E-01	2.34E-01	1.33E-01	2.43E-01	4.32E+00
		2.0	6.30E-01	2.83E-01	1.04E-01	7.38E-02	4.48E-01
	2.0	4.0	8.34E-01	3.95E-01	1.17E-01	2.71E-02	4.42E-02
		8.0	1.11E+00	5.79E-01	1.76E-01	1.63E-02	5.79E-03
		16.0	1.47E+00	8.45E-01	2.94E-01	2.00E-02	1.62E-03
		1.0	7.93E-01	4.92E-01	4.85E-01	3.69E+00	4.56E+02
		2.0	1.02E+00	5.73E-01	3.57E-01	1.12E+00	5.46E+01
	1.0	4.0	1.33E+00	7.47E-01	3.37E-01	3.36E-01	4.75E+00
		8.0	1.74E+00	1.03E+00	4.21E-01	1.32E-01	3.92E-01
		16.0	2.26E+00	1.43E+00	6.17E-01	9.79E-02	5.05E-02
		1.0	6.66E-01	3.62E-01	2.43E-01	6.72E-01	1.88E+01
		2.0	8.42E-01	4.36E-01	1.97E-01	2.14E-01	2.19E+00
2.0	1.5	4.0	1.09E+00	5.88E-01	2.17E-01	7.93E-02	2.30E-01
		8.0	1.43E+00	8.26E-01	3.08E-01	4.61E-02	3.00E-02
		16.0	1.85E+00	1.16E+00	4.80E-01	5.22E-02	7.82E-03
		1.0	5.81E-01	2.88E-01	1.46E-01	1.77E-01	1.40E+00
		2.0	7.33E-01	3.61E-01	1.33E-01	6.59E-02	1.98E-01
	2.0	4.0	9.49E-01	4.99E-01	1.65E-01	3.11E-02	2.86E-02
		8.0	1.24E+00	7.09E-01	2.52E-01	2.49E-02	5.90E-03
		16.0	1.60E+00	1.00E+00	4.05E-01	3.67E-02	2.66E-03

Table 1

$Q \equiv e^{E/T_o} dJ_o/d(E/T_o) \langle \sigma v \rangle_o H_o n_o a d0$

(= normalized flux $\cdot e^{E/T_o}$)

for $h^{-1} = .7\ \lambda_o^{-1}$

density profile: flat

Table 1 (continued)

density profile: cosine

T_o keV	ϑ	E_n/T_o	a/λ_o 1.	2.	4.	10.	20.
		1.0	6.15E-01	6.18E-01	2.26E+00	7.68E+02	6.04E+07
		2.0	8.56E-01	6.67E-01	1.42E+00	1.93E+02	5.42E+06
	1.0	4.0	1.18E+00	7.82E-01	8.79E-01	3.35E+01	2.26E+05
		8.0	1.60E+00	1.01E+00	6.69E-01	4.88E+00	4.73E+03
		16.0	2.13E+00	1.37E+00	7.12E-01	8.95E-01	7.33E+01
		1.0	5.47E-01	4.68E-01	1.20E+00	1.64E+02	3.41E+06
		2.0	7.28E-01	4.87E-01	6.80E-01	3.11E+01	1.79E+05
.3	1.5	4.0	9.81E-01	5.86E-01	4.39E-01	4.85E+00	5.23E+03
		8.0	1.32E+00	7.84E-01	3.96E-01	8.10E-01	1.06E+02
		16.0	1.75E+00	1.09E+00	4.95E-01	2.24E-01	2.46E+00
		1.0	4.90E-01	3.65E-01	6.85E-01	4.03E+01	2.35E+05
		2.0	6.40E-01	3.85E-01	3.86E-01	7.11E+00	1.02E+04
	2.0	4.0	8.56E-01	4.80E-01	2.75E-01	1.18E+00	2.91E+02
		8.0	1.15E+00	6.60E-01	2.87E-01	2.46E-01	7.30E+00
		16.0	1.52E+00	9.33E-01	3.95E-01	9.90E-02	2.79E-01
		1.0	6.96E-01	5.61E-01	1.08E+00	6.31E+01	2.29E+05
		2.0	9.83E-01	6.97E-01	8.49E-01	2.16E+01	3.21E+04
	1.0	4.0	1.35E+00	9.04E-01	7.07E-01	5.77E+00	2.49E+03
		8.0	1.81E+00	1.21E+00	7.21E-01	1.48E+00	1.21E+02
		16.0	2.36E+00	1.64E+00	9.00E-01	5.33E-01	5.60E+00
		1.0	6.35E-01	4.63E-01	6.81E-01	1.92E+01	2.41E+04
		2.0	8.53E-01	5.54E-01	4.97E-01	5.30E+00	2.21E+03
.7	1.5	4.0	1.14E+00	7.19E-01	4.36E-01	1.33E+00	1.34E+02
		8.0	1.50E+00	9.75E-01	4.98E-01	4.01E-01	6.87E+00
		16.0	1.95E+00	1.33E+00	6.78E-01	2.12E-01	4.85E-01
		1.0	5.81E-01	3.89E-01	4.49E-01	6.55E+00	3.01E+03
		2.0	7.61E-01	4.65E-01	3.32E-01	1.72E+00	2.41E+02
	2.0	4.0	1.00E+00	6.11E-01	3.16E-01	4.65E-01	1.49E+01
		8.0	1.31E+00	8.37E-01	3.93E-01	1.74E-01	9.53E-01
		16.0	1.69E+00	1.15E+00	5.62E-01	1.25E-01	1.05E-01
		1.0	7.45E-01	5.66E-01	8.36E-01	2.31E+01	2.35E+04
		2.0	1.05E+00	7.38E-01	7.31E-01	9.19E+00	4.05E+03
	1.0	4.0	1.44E+00	9.83E-01	6.95E-01	2.99E+00	4.18E+02
		8.0	1.91E+00	1.33E+00	7.85E-01	9.94E-01	3.01E+01
		16.0	2.48E+00	1.79E+00	1.02E+00	4.88E-01	2.28E+00
		1.0	6.85E-01	4.83E-01	5.64E-01	8.23E+00	3.24E+03
		2.0	9.19E-01	6.04E-01	4.67E-01	2.70E+00	3.86E+02
1.1	1.5	4.0	1.22E+00	7.98E-01	4.66E-01	8.47E-01	3.27E+01
		8.0	1.59E+00	1.08E+00	5.71E-01	3.36E-01	2.55E+00
		16.0	2.04E+00	1.46E+00	7.89E-01	2.33E-01	2.94E-01
		1.0	6.31E-01	4.17E-01	3.97E-01	3.23E+00	5.25E+02
		2.0	8.23E-01	5.18E-01	3.34E-01	1.02E+00	5.57E+01
	2.0	4.0	1.07E+00	6.86E-01	3.56E-01	3.45E-01	4.88E+00
		8.0	1.39E+00	9.31E-01	4.64E-01	1.69E-01	4.76E-01
		16.0	1.78E+00	1.26E+00	6.63E-01	1.52E-01	8.35E-02
		1.0	8.11E-01	5.95E-01	6.63E-01	8.05E+00	2.03E+03
		2.0	1.14E+00	8.07E-01	6.64E-01	3.81E+00	4.50E+02
	1.0	4.0	1.54E+00	1.10E+00	7.25E-01	1.58E+00	6.54E+01
		8.0	2.03E+00	1.48E+00	8.94E-01	7.18E-01	7.46E+00
		16.0	2.61E+00	1.97E+00	1.20E+00	4.95E-01	1.00E+00
		1.0	7.52E-01	5.23E-01	4.86E-01	3.40E+00	3.82E+02
		2.0	1.00E+00	6.79E-01	4.66E-01	1.37E+00	6.17E+01
2.0	1.5	4.0	1.31E+00	9.05E-01	5.26E-01	5.62E-01	7.78E+00
		8.0	1.70E+00	1.21E+00	6.82E-01	3.09E-01	9.91E-01
		16.0	2.16E+00	1.62E+00	9.45E-01	2.84E-01	2.01E-01
		1.0	6.97E-01	4.64E-01	3.68E-01	1.56E+00	8.30E+01
		2.0	9.02E-01	5.93E-01	3.58E-01	6.13E-01	1.22E+01
	2.0	4.0	1.16E+00	7.87E-01	4.22E-01	2.74E-01	1.61E+00
		8.0	1.49E+00	1.05E+00	5.68E-01	1.83E-01	2.56E-01
		16.0	1.88E+00	1.40E+00	8.04E-01	2.04E-01	7.63E-02

T_o keV	γ	E_n/T_o	a/λ_o 1.	2.	4.	10.	20.
		1.0	-1.99E-01	2.04E-01	8.32E-01	1.93E+00	3.18E+00
		2.0	-1.45E-01	-2.27E-02	3.65E-01	1.10E+00	1.94E+00
	1.0	4.0	-8.13E-02	-7.08E-02	8.60E-02	5.45E-01	1.10E+00
		8.0	-4.05E-02	-4.91E-02	-2.14E-02	2.11E-01	5.48E-01
		16.0	-1.93E-02	-2.56E-02	-2.89E-02	4.37E-02	2.19E-01
		1.0	-2.27E-01	1.05E-01	7.58E-01	1.93E+00	3.34E+00
		2.0	-1.57E-01	-9.36E-02	2.52E-01	9.90E-01	1.88E+00
.3	1.5	4.0	-8.47E-02	-9.54E-02	3.48E-03	4.30E-01	9.78E-01
		8.0	-4.14E-02	-5.50E-02	-5.19E-02	1.27E-01	4.34E-01
		16.0	-1.94E-02	-2.69E-02	-3.59E-02	3.01E-04	1.41E-01
		1.0	-2.58E-01	-8.64E-03	6.11E-01	1.72E+00	3.09E+00
		2.0	-1.66E-01	-1.45E-01	1.39E-01	8.28E-01	1.68E+00
	2.0	4.0	-8.69E-02	-1.10E-01	-5.48E-02	3.20E-01	8.23E-01
		8.0	-4.18E-02	-5.82E-02	-6.85E-02	6.24E-02	3.32E-01
		16.0	-1.95E-02	-2.75E-02	-3.93E-02	-2.61E-02	8.53E-02
		1.0	-2.42E-01	4.78E-03	5.89E-01	1.57E+00	2.66E+00
		2.0	-1.43E-01	-9.63E-02	1.99E-01	8.53E-01	1.58E+00
	1.0	4.0	-7.48E-02	-8.13E-02	1.50E-03	3.90E-01	8.62E-01
		8.0	-3.66E-02	-4.62E-02	-4.13E-02	1.22E-01	4.00E-01
		16.0	-1.74E-02	-2.28E-02	-2.89E-02	5.65E-03	1.38E-01
		1.0	-2.44E-01	-7.08E-02	5.04E-01	1.54E+00	2.75E+00
		2.0	-1.46E-01	-1.37E-01	9.18E-02	7.45E-01	1.51E+00
.7	1.5	4.0	-7.57E-02	-9.38E-02	-5.67E-02	2.84E-01	7.42E-01
		8.0	-3.68E-02	-4.92E-02	-5.82E-02	4.99E-02	2.97E-01
		16.0	-1.74E-02	-2.35E-02	-3.26E-02	-2.39E-02	7.42E-02
		1.0	-2.55E-01	-1.49E-01	3.67E-01	1.36E+00	2.53E+00
		2.0	-1.49E-01	-1.66E-01	-2.60E-03	6.05E-01	1.32E+00
	2.0	4.0	-7.63E-02	-1.01E-01	-9.33E-02	1.89E-01	6.06E-01
		8.0	-3.69E-02	-5.08E-02	-6.70E-02	-1.39E-03	2.11E-01
		16.0	-1.74E-02	-2.39E-02	-3.44E-02	-4.01E-02	3.05E-02
		1.0	-2.49E-01	-7.54E-02	4.66E-01	1.40E+00	2.42E+00
		2.0	-1.40E-01	-1.17E-01	1.20E-01	7.39E-01	1.42E+00
	1.0	4.0	-7.14E-02	-8.19E-02	-2.93E-02	3.19E-01	7.53E-01
		8.0	-3.47E-02	-4.42E-02	-4.57E-02	8.24E-02	3.33E-01
		16.0	-1.66E-02	-2.15E-02	-2.80E-02	-7.94E-03	1.03E-01
		1.0	-2.43E-01	-1.34E-01	3.74E-01	1.36E+00	2.48E+00
		2.0	-1.39E-01	-1.46E-01	2.13E-02	6.33E-01	1.33E+00
1.1	1.5	4.0	-7.14E-02	-9.05E-02	-7.45E-02	2.16E-01	6.34E-01
		8.0	-3.47E-02	-4.62E-02	-5.78E-02	1.74E-02	2.37E-01
		16.0	-1.65E-02	-2.20E-02	-3.06E-02	-3.08E-02	4.64E-02
		1.0	-2.46E-01	-1.93E-01	2.43E-01	1.19E+00	2.27E+00
		2.0	-1.40E-01	-1.66E-01	-5.89E-02	5.02E-01	1.16E+00
	2.0	4.0	-7.16E-02	-9.54E-02	-1.02E-01	1.28E-01	5.08E-01
		8.0	-3.47E-02	-4.73E-02	-6.41E-02	-2.60E-02	1.59E-01
		16.0	-1.65E-02	-2.22E-02	-3.19E-02	-4.26E-02	8.25E-03
		1.0	-2.50E-01	-1.52E-01	3.06E-01	1.19E+00	2.12E+00
		2.0	-1.34E-01	-1.32E-01	2.99E-02	6.03E-01	1.22E+00
	1.0	4.0	-6.71E-02	-8.02E-02	-5.61E-02	2.33E-01	6.24E-01
		8.0	-3.26E-02	-4.14E-02	-4.77E-02	3.78E-02	2.56E-01
		16.0	-1.56E-02	-2.00E-02	-2.64E-02	-1.96E-02	6.49E-02
		1.0	-2.35E-01	-1.87E-01	2.12E-01	1.14E+00	2.15E+00
		2.0	-1.30E-01	-1.49E-01	-5.02E-02	4.97E-01	1.13E+00
2.0	1.5	4.0	-6.64E-02	-8.51E-02	-8.69E-02	1.35E-01	5.09E-01
		8.0	-3.24E-02	-4.26E-02	-5.55E-02	-1.56E-02	1.68E-01
		16.0	-1.56E-02	-2.02E-02	-2.81E-02	-3.51E-02	1.65E-02
		1.0	-2.31E-01	-2.25E-01	9.36E-02	9.90E-01	1.96E+00
		2.0	-1.29E-01	-1.61E-01	-1.11E-01	3.76E-01	9.66E-01
	2.0	4.0	-6.61E-02	-8.80E-02	-1.05E-01	5.54E-02	3.95E-01
		8.0	-3.23E-02	-4.32E-02	-5.95E-02	-4.83E-02	9.95E-02
		16.0	-1.55E-02	-2.04E-02	-2.89E-02	-4.28E-02	-1.44E-02

Table 2

$R \equiv T_o/T_{\phi_n} - 1$; $T_{\phi_n}^{-1} = E_n^{-1} \ln \frac{J_o(E_n)}{J_o(2E_n)}$

(= relative correction for T_o if this quantity is derived from the logarithmic slope of the flux spectrum between energies E_n and 2 E_n)

for $h^{-1} = .7\lambda_o^{-1}$

density profile: flat

Table 2 (continued)

density profile: cosine

T_o keV	ϑ	E_n/T_o	a/r_o 1.	2.	4.	10.	20.
		1.0	-3.31E-01	-7.57E-02	4.65E-01	1.38E+00	2.41E+00
		2.0	-1.60E-01	-7.97E-02	2.40E-01	8.75E-01	1.59E+00
	1.0	4.0	-7.61E-02	-6.34E-02	6.81E-02	4.82E-01	9.66E-01
		8.0	-3.58E-02	-3.83E-02	-7.71E-03	2.12E-01	5.21E-01
		16.0	-1.67E-02	-1.98E-02	-1.79E-02	5.94E-02	2.30E-01
		1.0	-2.85E-01	-3.98E-02	5.71E-01	1.66E+00	2.95E+00
		2.0	-1.49E-01	-9.26E-02	2.19E-01	9.30E-01	1.77E+00
.3	1.5	4.0	-7.37E-02	-7.27E-02	2.57E-02	4.48E-01	9.76E-01
		8.0	-3.52E-02	-4.13E-02	-2.78E-02	1.60E-01	4.70E-01
		16.0	-1.66E-02	-2.06E-02	-2.33E-02	2.54E-02	1.77E-01
		1.0	-2.67E-01	-5.31E-02	5.73E-01	1.74E+00	3.14E+00
		2.0	-1.46E-01	-1.10E-01	1.70E-01	8.99E-01	1.78E+00
	2.0	4.0	-7.29E-02	-7.96E-02	-1.01E-02	3.91E-01	9.21E-01
		8.0	-3.49E-02	-4.32E-02	-4.00E-02	1.14E-01	4.08E-01
		16.0	-1.65E-02	-2.10E-02	-2.62E-02	3.12E-03	1.33E-01
		1.0	-3.45E-01	-2.16E-01	2.45E-01	1.07E+00	1.97E+00
		2.0	-1.59E-01	-1.30E-01	9.15E-02	6.61E-01	1.28E+00
	1.0	4.0	-7.29E-02	-7.35E-02	-4.90E-03	3.41E-01	7.55E-01
		8.0	-3.36E-02	-3.81E-02	-2.78E-02	1.27E-01	3.84E-01
		16.0	-1.56E-02	-1.86E-02	-2.03E-02	2.05E-02	1.52E-01
		1.0	-2.95E-01	-1.79E-01	3.15E-01	1.29E+00	2.39E+00
		2.0	-1.45E-01	-1.30E-01	6.48E-02	6.90E-01	1.40E+00
.7	1.5	4.0	-6.90E-02	-7.61E-02	-3.31E-02	3.00E-01	7.44E-01
		8.0	-3.26E-02	-3.91E-02	-3.84E-02	7.95E-02	3.31E-01
		16.0	-1.54E-02	-1.89E-02	-2.30E-02	-2.96E-03	1.06E-01
		1.0	-2.70E-01	-1.78E-01	3.02E-01	1.34E+00	2.53E+00
		2.0	-1.38E-01	-1.36E-01	2.37E-02	6.54E-01	1.39E+00
	2.0	4.0	-6.72E-02	-7.85E-02	-5.45E-02	2.46E-01	6.87E-01
		8.0	-3.21E-02	-3.97E-02	-4.46E-02	4.13E-02	2.75E-01
		16.0	-1.52E-02	-1.90E-02	-2.44E-02	-1.66E-02	7.01E-02
		1.0	-3.45E-01	-2.65E-01	1.34E-01	9.24E-01	1.76E+00
		2.0	-1.56E-01	-1.43E-01	2.54E-02	5.61E-01	1.14E+00
	1.0	4.0	-7.10E-02	-7.51E-02	-3.04E-02	2.75E-01	6.58E-01
		8.0	-3.26E-02	-3.73E-02	-3.31E-02	8.89E-02	3.22E-01
		16.0	-1.52E-02	-1.79E-02	-2.04E-02	6.25E-03	1.18E-01
		1.0	-2.94E-01	-2.24E-01	1.89E-01	1.12E+00	2.13E+00
		2.0	-1.41E-01	-1.39E-01	1.45E-03	5.79E-01	1.23E+00
1.1	1.5	4.0	-6.67E-02	-7.55E-02	-5.11E-02	2.31E-01	6.38E-01
		8.0	-3.14E-02	-3.76E-02	-4.03E-02	4.54E-02	2.70E-01
		16.0	-1.48E-02	-1.80E-02	-2.23E-02	-1.18E-02	7.54E-02
		1.0	-2.66E-01	-2.16E-01	1.73E-01	1.15E+00	2.24E+00
		2.0	-1.33E-01	-1.41E-01	-3.19E-02	5.41E-01	1.22E+00
	2.0	4.0	-6.45E-02	-7.64E-02	-6.64E-02	1.79E-01	5.82E-01
		8.0	-3.08E-02	-3.79E-02	-4.46E-02	1.29E-02	2.18E-01
		16.0	-1.47E-02	-1.81E-02	-2.33E-02	-2.18E-02	4.40E-02
		1.0	-3.40E-01	-3.05E-01	-1.00E-03	7.49E-01	1.51E+00
		2.0	-1.52E-01	-1.53E-01	-4.37E-02	4.41E-01	9.64E-01
	1.0	4.0	-6.85E-02	-7.50E-02	-5.24E-02	1.96E-01	5.43E-01
		8.0	-3.14E-02	-3.61E-02	-3.65E-02	4.64E-02	2.51E-01
		16.0	-1.46E-02	-1.71E-02	-2.01E-02	-6.48E-03	7.99E-02
		1.0	-2.88E-01	-2.60E-01	4.10E-02	9.09E-01	1.82E+00
		2.0	-1.36E-01	-1.44E-01	-6.01E-02	4.46E-01	1.04E+00
2.0	1.5	4.0	-6.38E-02	-7.34E-02	-6.51E-02	1.50E-01	5.15E-01
		8.0	-3.01E-02	-3.58E-02	-4.08E-02	1.06E-02	2.00E-01
		16.0	-1.43E-02	-1.70E-02	-2.12E-02	-1.87E-02	4.25E-02
		1.0	-2.58E-01	-2.45E-01	2.72E-02	9.37E-01	1.91E+00
		2.0	-1.27E-01	-1.41E-01	-8.26E-02	4.04E-01	1.01E+00
	2.0	4.0	-6.13E-02	-7.31E-02	-7.44E-02	1.00E-01	4.60E-01
		8.0	-2.94E-02	-3.57E-02	-4.34E-02	-1.38E-02	1.51E-01
		16.0	-1.41E-02	-1.70E-02	-2.18E-02	-2.52E-02	1.67E-02

T_o keV	ϑ	E_n/T_o	a/λ_o = 1.	2.	4.	10.	20.
		1.0	6.67E-01	1.34E+00	8.68E+00	3.62E+04	2.91E+11
		2.0	7.41E-01	6.96E-01	2.95E+00	3.54E+03	6.52E+09
	1.0	4.0	9.24E-01	5.76E-01	9.97E-01	2.26E+02	6.45E+07
		8.0	1.23E+00	6.39E-01	4.49E-01	1.18E+01	2.56E+05
		16.0	1.66E+00	8.56E-01	3.54E-01	8.16E-01	6.71E+02
		1.0	4.77E-01	4.92E-01	1.97E+00	1.20E+03	6.18E+08
		2.0	5.52E-01	3.57E-01	6.95E-01	1.08E+02	1.05E+07
.3	1.5	4.0	7.16E-01	3.50E-01	2.86E-01	7.89E+00	9.15E+04
		8.0	9.75E-01	4.49E-01	1.83E-01	6.24E-01	5.04E+02
		16.0	1.34E+00	6.50E-01	2.05E-01	8.77E-02	3.07E+00
		1.0	3.73E-01	2.81E-01	6.22E-01	7.36E+01	3.08E+06
		2.0	4.51E-01	2.30E-01	2.51E-01	7.85E+00	6.13E+04
	2.0	4.0	6.02E-01	2.57E-01	1.29E-01	7.72E-01	7.46E+02
		8.0	8.33E-01	3.59E-01	1.09E-01	9.57E-02	7.34E+00
		16.0	1.15E+00	5.43E-01	1.49E-01	2.38E-02	1.05E-01
		1.0	7.24E-01	7.51E-01	2.86E+00	1.04E+03	1.13E+08
		2.0	8.73E-01	6.32E-01	1.27E+00	1.55E+02	4.88E+06
	1.0	4.0	1.12E+00	6.56E-01	6.19E-01	1.74E+01	1.03E+05
		8.0	1.47E+00	8.19E-01	4.33E-01	1.91E+00	1.23E+03
		16.0	1.95E+00	1.12E+00	4.71E-01	3.22E-01	1.36E+01
		1.0	5.64E-01	4.32E-01	9.11E-01	7.25E+01	8.58E+05
		2.0	6.88E-01	3.94E-01	4.27E-01	1.04E+01	2.96E+04
.7	1.5	4.0	8.94E-01	4.57E-01	2.55E-01	1.37E+00	6.39E+02
		8.0	1.19E+00	6.18E-01	2.38E-01	2.24E-01	1.12E+01
		16.0	1.58E+00	8.81E-01	3.18E-01	7.08E-02	2.79E-01
		1.0	4.68E-01	2.89E-01	3.80E-01	8.47E+00	1.40E+04
		2.0	5.81E-01	2.89E-01	2.01E-01	1.42E+00	5.63E+02
	2.0	4.0	7.65E-01	3.63E-01	1.48E-01	2.44E-01	1.68E+01
		8.0	1.02E+00	5.13E-01	1.68E-01	5.91E-02	4.99E-01
		16.0	1.37E+00	7.48E-01	2.51E-01	3.01E-02	2.59E-02
		1.0	7.74E-01	6.90E-01	1.87E+00	2.50E+02	4.54E+06
		2.0	9.53E-01	6.45E-01	9.45E-01	4.53E+01	2.59E+05
	1.0	4.0	1.23E+00	7.24E-01	5.54E-01	6.63E+00	8.00E+03
		8.0	1.60E+00	9.32E-01	4.66E-01	1.02E+00	1.60E+02
		16.0	2.09E+00	1.27E+00	5.59E-01	2.57E-01	3.41E+00
		1.0	6.22E-01	4.33E-01	6.90E-01	2.40E+01	6.05E+04
		2.0	7.66E-01	4.34E-01	3.73E-01	4.27E+00	2.90E+03
1.1	1.5	4.0	9.90E-01	5.29E-01	2.66E-01	7.39E-01	9.51E+01
		8.0	1.30E+00	7.19E-01	2.85E-01	1.68E-01	2.83E+00
		16.0	1.71E+00	1.01E+00	3.98E-01	7.59E-02	1.32E-01
		1.0	5.27E-01	3.09E-01	3.25E-01	3.70E+00	1.64E+03
		2.0	6.55E-01	3.33E-01	1.98E-01	7.61E-01	9.18E+01
	2.0	4.0	8.52E-01	4.30E-01	1.70E-01	1.70E-01	4.11E+00
		8.0	1.12E+00	6.04E-01	2.12E-01	5.57E-02	2.02E-01
		16.0	1.47E+00	8.64E-01	3.22E-01	3.85E-02	1.85E-02
		1.0	8.53E-01	6.64E-01	1.22E+00	5.51E+01	1.43E+05
		2.0	1.06E+00	6.94E-01	7.31E-01	1.26E+01	1.15E+04
	1.0	4.0	1.36E+00	8.32E-01	5.34E-01	2.53E+00	5.59E+02
		8.0	1.76E+00	1.09E+00	5.40E-01	5.82E-01	2.06E+01
		16.0	2.27E+00	1.48E+00	6.99E-01	2.34E-01	9.42E-01
		1.0	7.05E-01	4.58E-01	5.35E-01	7.61E+00	3.63E+03
		2.0	8.71E-01	5.02E-01	3.46E-01	1.75E+00	2.56E+02
2.0	1.5	4.0	1.11E+00	6.34E-01	3.02E-01	4.17E-01	1.38E+01
		8.0	1.44E+00	8.60E-01	3.64E-01	1.40E-01	7.62E-01
		16.0	1.86E+00	1.19E+00	5.21E-01	9.42E-02	7.23E-02
		1.0	6.38E-01	3.49E-01	2.88E-01	1.60E+00	1.75E+02
		2.0	7.52E-01	4.03E-01	2.10E-01	4.20E-01	1.44E+01
	2.0	4.0	9.63E-01	5.28E-01	2.13E-01	1.27E-01	1.04E+00
		8.0	1.25E+00	7.31E-01	2.86E-01	5.99E-02	9.10E-02
		16.0	1.61E+00	1.02E+00	4.31E-01	5.68E-02	1.58E-02

Table 1a

$Q \equiv e^{E/T_o} dJ_o/d(E/T_o) \; \langle \sigma v \rangle_o \; H_o n_o a dO$

(= normalized flux · e^{E/T_o})

for $h^{-1} = 1.0 \; \lambda_o^{-1}$

density profile: flat

Table 1a (continued)

density profile: cosine

T_o / keV	ϑ	E_n/T_o	a/λ_o = 1.	2.	4.	10.	20.
		1.0	7.39E-01	1.21E+00	1.26E+01	1.04E+05	2.09E+12
		2.0	5.68E-01	1.10E+00	6.26E+00	1.77E+04	1.05E+11
	1.0	4.0	1.27E+00	1.08E+00	2.80E+00	1.79E+03	1.94E+09
		8.0	1.67E+00	1.21E+00	1.44E+00	1.28E+02	1.35E+07
		16.0	2.18E+00	1.51E+00	1.08E+00	9.67E+00	4.89E+04
		1.0	6.39E-01	8.42E-01	5.69E+00	1.48E+04	5.49E+10
		2.0	8.02E-01	7.29E-01	2.45E+00	1.76E+03	1.39E+09
.3	1.5	4.0	1.04E+00	7.44E-01	1.12E+00	1.50E+02	1.58E+07
		8.0	1.36E+00	8.91E-01	6.90E-01	1.18E+01	9.43E+04
		16.0	1.77E+00	1.17E+00	6.57E-01	1.37E+00	4.85E+02
		1.0	5.59E-01	6.10E-01	2.80E+00	2.54E+03	1.90E+09
		2.0	6.93E-01	5.38E-01	1.19E+00	2.73E+02	3.69E+07
	2.0	4.0	8.95E-01	5.80E-01	5.95E-01	2.43E+01	3.86E+05
		8.0	1.17E+00	7.28E-01	4.40E-01	2.40E+00	2.79E+03
		16.0	1.53E+00	9.81E-01	4.88E-01	4.19E-01	2.41E+01
		1.0	7.72E-01	8.53E-01	3.68E+00	2.33E+03	5.36E+08
		2.0	1.05E+00	9.34E-01	2.33E+00	5.71E+02	4.56E+07
	1.0	4.0	1.41E+00	1.08E+00	1.47E+00	9.68E+01	1.78E+06
		8.0	1.85E+00	1.34E+00	1.12E+00	1.37E+01	3.43E+04
		16.0	2.40E+00	1.74E+00	1.14E+00	2.41E+00	4.78E+02
		1.0	6.93E-01	6.62E-01	2.03E+00	5.16E+02	3.09E+07
		2.0	9.01E-01	6.98E-01	1.17E+00	9.65E+01	1.55E+06
.7	1.5	4.0	1.18E+00	8.22E-01	7.67E-01	1.48E+01	4.27E+04
		8.0	1.53E+00	1.05E+00	6.81E-01	2.39E+00	7.99E+02
		16.0	1.97E+00	1.38E+00	7.94E-01	6.35E-01	1.67E+01
		1.0	6.25E-01	5.30E-01	1.20E+00	1.34E+02	2.27E+06
		2.0	7.95E-01	5.62E-01	6.89E-01	2.34E+01	9.39E+04
	2.0	4.0	1.03E+00	6.79E-01	4.98E-01	3.79E+00	2.54E+03
		8.0	1.33E+00	8.85E-01	5.00E-01	7.66E-01	5.87E+01
		16.0	1.71E+00	1.18E+00	6.34E-01	2.91E-01	1.99E+00
		1.0	8.05E-01	7.79E-01	2.29E+00	4.97E+02	1.79E+07
		2.0	1.11E+00	9.18E-01	1.64E+00	1.45E+02	1.95E+06
	1.0	4.0	1.48E+00	1.12E+00	1.22E+00	3.12E+01	1.07E+05
		8.0	1.94E+00	1.43E+00	1.09E+00	6.04E+00	3.31E+03
		16.0	2.50E+00	1.86E+00	1.21E+00	1.56E+00	8.53E+01
		1.0	7.31E-01	6.32E-01	1.38E+00	1.34E+02	1.45E+06
		2.0	9.57E-01	7.17E-01	9.14E-01	3.08E+01	9.94E+04
1.1	1.5	4.0	1.25E+00	8.81E-01	7.12E-01	6.16E+00	4.13E+03
		8.0	1.61E+00	1.14E+00	7.19E-01	1.39E+00	1.30E+02
		16.0	2.06E+00	1.50E+00	8.87E-01	5.32E-01	5.08E+00
		1.0	6.67E-01	5.26E-01	8.83E-01	4.16E+01	1.48E+05
		2.0	8.51E-01	5.96E-01	5.89E-01	9.04E+00	8.64E+03
	2.0	4.0	1.09E+00	7.42E-01	4.99E-01	1.93E+00	3.59E+02
		8.0	1.40E+00	9.71E-01	5.54E-01	5.40E-01	1.40E+01
		16.0	1.79E+00	1.29E+00	7.25E-01	2.86E-01	8.68E-01
		1.0	8.55E-01	7.41E-01	1.43E+00	9.58E+01	4.54E+05
		2.0	1.18E+00	9.37E-01	1.20E+00	3.44E+01	6.65E+04
	1.0	4.0	1.58E+00	1.20E+00	1.07E+00	9.83E+00	5.52E+03
		8.0	2.06E+00	1.56E+00	1.11E+00	2.76E+00	2.98E+02
		16.0	2.63E+00	2.03E+00	1.34E+00	1.11E+00	1.57E+01
		1.0	7.86E-01	6.30E-01	9.55E-01	3.22E+01	5.46E+04
		2.0	1.03E+00	7.63E-01	7.53E-01	9.47E+00	5.41E+03
2.0	1.5	4.0	1.34E+00	9.68E-01	7.02E-01	2.59E+00	3.62E+02
		8.0	1.71E+00	1.26E+00	7.96E-01	8.66E-01	2.09E+01
		16.0	2.17E+00	1.65E+00	1.02E+00	4.97E-01	1.67E+00
		1.0	7.24E-01	5.44E-01	6.68E-01	1.22E+01	8.04E+03
		2.0	9.23E-01	6.52E-01	5.34E-01	3.44E+00	7.02E+02
	2.0	4.0	1.18E+00	8.30E-01	5.30E-01	1.01E+00	4.82E+01
		8.0	1.50E+00	1.08E+00	6.40E-01	4.17E-01	3.46E+00
		16.0	1.89E+00	1.42E+00	8.54E-01	3.12E-01	4.23E-01

T_o keV	ϑ	E_n/T_o	a/λ_o = 1.	2.	4.	10.	20.
		1.0	-1.05E-01	4.06E-01	1.08E+00	2.32E+00	3.74E+00
		2.0	-1.10E-01	9.41E-02	5.42E-01	1.38E+00	2.34E+00
	1.0	4.0	-7.08E-02	-2.60E-02	2.00E-01	7.39E-01	1.38E+00
		8.0	-3.77E-02	-3.65E-02	7.94E-02	3.34E-01	7.43E-01
		16.0	-1.85E-02	-2.24E-02	-1.44E-02	1.09E-01	3.40E-01
		1.0	-1.45E-01	3.20E-01	1.04E+00	2.41E+00	4.07E+00
		2.0	-1.30E-01	9.85E-03	4.44E-01	1.31E+00	2.37E+00
.3	1.5	4.0	-7.72E-02	-6.21E-02	1.11E-01	6.34E-01	1.30E+00
		8.0	-3.94E-02	-4.64E-02	-1.36E-02	2.45E-01	6.38E-01
		16.0	-1.89E-02	-2.47E-02	-2.62E-02	5.56E-02	2.55E-01
		1.0	-1.88E-01	2.02E-01	9.08E-01	2.24E+00	3.92E+00
		2.0	-1.45E-01	-5.66E-02	3.32E-01	1.16E+00	2.20E+00
	2.0	4.0	-8.10E-02	-8.36E-02	4.13E-02	5.22E-01	1.16E+00
		8.0	-4.03E-02	-5.16E-02	-3.88E-02	1.74E-01	5.31E-01
		16.0	-1.91E-02	-2.59E-02	-3.22E-02	2.06E-02	1.90E-01
		1.0	-1.86E-01	1.72E-01	8.12E-01	1.91E+00	3.14E+00
		2.0	-1.24E-01	-1.86E-02	3.58E-01	1.09E+00	1.93E+00
	1.0	4.0	-6.90E-02	-5.57E-02	8.96E-02	5.54E-01	1.11E+00
		8.0	-3.49E-02	-3.92E-02	-1.05E-02	2.22E-01	5.63E-01
		16.0	-1.70E-02	-2.10E-02	-2.10E-02	5.29E-02	2.33E-01
		1.0	-1.98E-01	9.18E-02	7.58E-01	1.94E+00	3.37E+00
		2.0	-1.31E-01	-7.41E-02	2.57E-01	1.01E+00	1.92E+00
.7	1.5	4.0	-7.15E-02	-7.53E-02	1.77E-02	4.53E-01	1.01E+00
		8.0	-3.56E-02	-4.44E-02	-3.64E-02	1.44E-01	4.62E-01
		16.0	-1.71E-02	-2.23E-02	-2.73E-02	1.28E-02	1.61E-01
		1.0	-2.16E-01	-5.31E-04	6.34E-01	1.79E+00	3.21E+00
		2.0	-1.37E-01	-1.14E-01	1.56E-01	8.79E-01	1.76E+00
	2.0	4.0	-7.31E-02	-8.67E-02	-3.17E-02	3.55E-01	8.79E-01
		8.0	-3.60E-02	-4.71E-02	-5.05E-02	8.45E-02	3.70E-01
		16.0	-1.72E-02	-2.29E-02	-3.05E-02	-1.11E-02	1.09E-01
		1.0	-2.08E-01	6.70E-02	6.80E-01	1.71E+00	2.86E+00
		2.0	-1.25E-01	-5.77E-02	2.67E-01	9.61E-01	1.74E+00
	1.0	4.0	-6.71E-02	-6.31E-02	4.33E-02	4.68E-01	9.78E-01
		8.0	-3.35E-02	-3.90E-02	-2.27E-02	1.72E-01	4.81E-01
		16.0	-1.62E-02	-2.02E-02	-2.22E-02	3.05E-02	1.87E-01
		1.0	-2.08E-01	-1.65E-03	6.17E-01	1.73E+00	3.04E+00
		2.0	-1.28E-01	-9.90E-02	1.68E-01	8.77E-01	1.71E+00
1.1	1.5	4.0	-6.83E-02	-7.69E-02	-1.65E-02	3.70E-01	8.78E-01
		8.0	-3.39E-02	-4.27E-02	-4.19E-02	9.94E-02	3.84E-01
		16.0	-1.63E-02	-2.11E-02	-2.67E-02	-2.38E-03	1.22E-01
		1.0	-2.17E-01	-7.59E-02	4.95E-01	1.58E+00	2.89E+00
		2.0	-1.32E-01	-1.28E-01	7.59E-02	7.51E-01	1.55E+00
	2.0	4.0	-6.91E-02	-8.49E-02	-5.51E-02	2.78E-01	7.54E-01
		8.0	-3.41E-02	-4.46E-02	-5.21E-02	4.63E-02	2.99E-01
		16.0	-1.64E-02	-2.15E-02	-2.90E-02	-2.09E-02	7.54E-02
		1.0	-2.22E-01	-4.36E-02	5.11E-01	1.47E+00	2.53E+00
		2.0	-1.24E-01	-9.11E-02	1.58E-01	8.04E-01	1.51E+00
	1.0	4.0	-6.42E-02	-6.76E-02	-2.79E-03	3.67E-01	8.25E-01
		8.0	-3.18E-02	-3.79E-02	-3.23E-02	1.14E-01	3.86E-01
		16.0	-1.54E-02	-1.91E-02	-2.25E-02	8.30E-03	1.35E-01
		1.0	-2.11E-01	-9.17E-02	4.36E-01	1.47E+00	2.65E+00
		2.0	-1.23E-01	-1.17E-01	6.72E-02	7.16E-01	1.46E+00
2.0	1.5	4.0	-6.42E-02	-7.60E-02	-4.65E-02	2.72E-01	7.24E-01
		8.0	-3.18E-02	-4.02E-02	-4.49E-02	4.99E-02	2.94E-01
		16.0	-1.54E-02	-1.96E-02	-2.54E-02	-1.56E-02	7.81E-02
		1.0	-2.12E-01	-1.43E-01	3.18E-01	1.34E+00	2.50E+00
		2.0	-1.23E-01	-1.36E-01	-7.86E-03	5.99E-01	1.31E+00
	2.0	4.0	-6.44E-02	-8.10E-02	-7.32E-02	1.87E-01	6.09E-01
		8.0	-3.19E-02	-4.14E-02	-5.15E-02	6.57E-03	2.19E-01
		16.0	-1.54E-02	-1.99E-02	-2.70E-02	-2.83E-02	3.90E-02

Table 2a

$R \equiv T_o/T_\phi - 1$; $T_\phi^{-1} = E_n^{-1} \ln \frac{J_o(E_n)}{J_o(2E_n)}$

(= relative correction for T_o if this quantity is derived from the logarithmic slope of the flux spectrum between energies E_n and 2 E_n)

for $h^{-1} = 1.0\ \lambda_o^{-1}$

density profile: flat

Table 2a (continued)

density profile: cosine

T_o / keV	ϑ	E_n/T_o	a/λ_o 1.	2.	4.	10.	20.
		1.0	-2.70E-01	9.73E-02	7.01E-01	1.78E+00	3.00E+00
		2.0	-1.36E-01	9.92E-03	4.01E-01	1.14E+00	1.99E+00
	1.0	4.0	-6.80E-02	-2.86E-02	1.67E-01	6.60E-01	1.24E+00
		8.0	-3.33E-02	-2.76E-02	3.58E-02	3.23E-01	7.03E-01
		16.0	-1.60E-02	-1.69E-02	-4.91E-03	1.19E-01	3.42E-01
		1.0	-2.27E-01	1.44E-01	8.40E-01	2.13E+00	3.68E+00
		2.0	-1.29E-01	-1.01E-02	3.94E-01	1.23E+00	2.24E+00
.3	1.5	4.0	-6.74E-02	-4.51E-02	1.20E-01	6.35E-01	1.28E+00
		8.0	-3.34E-02	-3.36E-02	6.15E-03	2.69E-01	6.59E-01
		16.0	-1.61E-02	-1.86E-02	-1.44E-02	7.70E-02	2.83E-01
		1.0	-2.14E-01	1.27E-01	8.56E-01	2.23E+00	3.94E+00
		2.0	-1.28E-01	-3.75E-02	3.47E-01	1.21E+00	2.28E+00
	2.0	4.0	-6.77E-02	-5.72E-02	7.52E-02	5.79E-01	1.23E+00
		8.0	-3.35E-02	-3.72E-02	-1.29E-02	2.18E-01	5.94E-01
		16.0	-1.61E-02	-1.95E-02	-1.94E-02	4.73E-02	2.32E-01
		1.0	-3.11E-01	-9.08E-02	4.57E-01	1.40E+00	2.46E+00
		2.0	-1.45E-01	-7.43E-02	2.31E-01	8.87E-01	1.62E+00
	1.0	4.0	-6.83E-02	-5.38E-02	6.75E-02	4.89E-01	9.87E-01
		8.0	-3.22E-02	-3.21E-02	-1.81E-03	2.17E-01	5.34E-01
		16.0	-1.52E-02	-1.70E-02	-1.31E-02	6.34E-02	2.39E-01
		1.0	-2.62E-01	-5.31E-02	5.55E-01	1.68E+00	2.99E+00
		2.0	-1.33E-01	-8.17E-02	2.09E-01	9.39E-01	1.79E+00
.7	1.5	4.0	-6.55E-02	-6.08E-02	2.99E-02	4.55E-01	9.95E-01
		8.0	-3.16E-02	-3.48E-02	-1.92E-02	1.66E-01	4.83E-01
		16.0	-1.51E-02	-1.77E-02	-1.80E-02	3.12E-02	1.87E-01
		1.0	-2.41E-01	-5.98E-02	5.53E-01	1.75E+00	3.19E+00
		2.0	-1.28E-01	-9.44E-02	1.63E-01	9.09E-01	1.81E+00
	2.0	4.0	-6.43E-02	-6.61E-02	-1.03E-03	4.00E-01	9.42E-01
		8.0	-3.13E-02	-3.63E-02	-2.97E-02	1.21E-01	4.23E-01
		16.0	-1.50E-02	-1.81E-02	-2.07E-02	1.08E-02	1.44E-01
		1.0	-3.20E-01	-1.64E-01	3.35E-01	1.23E+00	2.22E+00
		2.0	-1.46E-01	-1.01E-01	1.50E-01	7.68E-01	1.45E+00
	1.0	4.0	-6.76E-02	-6.05E-02	2.77E-02	4.11E-01	8.69E-01
		8.0	-3.16E-02	-3.30E-02	-1.37E-02	1.69E-01	4.57E-01
		16.0	-1.49E-02	-1.67E-02	-1.51E-02	4.10E-02	1.95E-01
		1.0	-2.69E-01	-1.26E-01	4.13E-01	1.47E+00	2.68E+00
		2.0	-1.32E-01	-1.03E-01	1.25E-01	8.06E-01	1.59E+00
1.1	1.5	4.0	-6.40E-02	-6.42E-02	-2.61E-03	3.72E-01	8.65E-01
		8.0	-3.07E-02	-3.44E-02	-2.62E-02	1.20E-01	4.05E-01
		16.0	-1.46E-02	-1.72E-02	-1.86E-02	1.45E-02	1.46E-01
		1.0	-2.44E-01	-1.25E-01	4.04E-01	1.53E+00	2.84E+00
		2.0	-1.26E-01	-1.10E-01	8.36E-02	7.73E-01	1.59E+00
	2.0	4.0	-6.23E-02	-6.73E-02	-2.61E-02	3.18E-01	8.10E-01
		8.0	-3.02E-02	-3.54E-02	-3.37E-02	7.96E-02	3.48E-01
		16.0	-1.45E-02	-1.74E-02	-2.05E-02	-1.30E-03	1.07E-01
		1.0	-3.23E-01	-2.34E-01	1.81E-01	1.02E+00	1.92E+00
		2.0	-1.45E-01	-1.24E-01	5.73E-02	6.26E-01	1.24E+00
	1.0	4.0	-6.62E-02	-6.52E-02	-1.08E-02	3.17E-01	7.30E-01
		8.0	-3.07E-02	-3.31E-02	-2.35E-02	1.14E-01	3.68E-01
		16.0	-1.44E-02	-1.63E-02	-1.65E-02	1.86E-02	1.44E-01
		1.0	-2.71E-01	-1.91E-01	2.38E-01	1.22E+00	2.31E+00
		2.0	-1.30E-01	-1.19E-01	3.51E-02	6.48E-01	1.35E+00
2.0	1.5	4.0	-6.20E-02	-6.58E-02	-3.16E-02	2.74E-01	7.13E-01
		8.0	-2.95E-02	-3.36E-02	-3.14E-02	6.95E-02	3.16E-01
		16.0	-1.41E-02	-1.64E-02	-1.87E-02	-5.85E-04	1.00E-01
		1.0	-2.43E-01	-1.81E-01	2.24E-01	1.27E+00	2.44E+00
		2.0	-1.22E-01	-1.20E-01	2.99E-03	6.11E-01	1.34E+00
	2.0	4.0	-5.99E-02	-6.69E-02	-4.71E-02	2.22E-01	6.58E-01
		8.0	-2.90E-02	-3.40E-02	-3.60E-02	3.64E-02	2.63E-01
		16.0	-1.40E-02	-1.65E-02	-1.99E-02	-1.14E-02	6.72E-02

Table 3: Summary of expressions for the atomic flux

energy range	normalized, attenuated source	normalized flux spectrum (radial emission)	Eq.
	$\frac{A_+}{A_\circ}\frac{H}{H_\circ}\frac{n}{n_\circ}\left(\frac{T}{T_\circ}\right)^{-3/2} e^{-E/T}$	$dJ_\circ/d\varepsilon \langle\sigma v\rangle_\circ H_\circ n_\circ a\, d\Omega$, $\varepsilon \equiv \frac{E}{T_\circ}$	
$\varepsilon \gg 1$	$e^{-\frac{\varepsilon-\varepsilon_1}{2\,\lvert t\rvert^2} r^2 - \varepsilon}$	$2^{3/2}\frac{\lvert t\rvert}{a}\varepsilon^{1/4}\left(\frac{\varepsilon}{\varepsilon-\varepsilon_1}\right)^{1/2} e^{-g-\varepsilon}$; $\varepsilon_1 \equiv \frac{3}{2} - \frac{t^2}{h^2} - \frac{t^2}{\lambda^2} - \frac{t^2}{d^2}$	(9)
$\gg 1$	$Ch\frac{r}{\lambda_\circ} Ch\frac{r}{h} e^{-\frac{\varepsilon-\varepsilon_2}{2\,\lvert t\rvert^2} r^2 - \varepsilon}$	$2^{3/2}\frac{\lvert t\rvert}{a}\varepsilon^{1/4}\left(\frac{\varepsilon}{\varepsilon-\varepsilon_2}\right)^{1/2} \frac{e^{\frac{\varkappa_+^2/2}{\varepsilon-\varepsilon_2}} + e^{\frac{\varkappa_-^2/2}{\varepsilon-\varepsilon_2}}}{2} e^{-g-\varepsilon}$ $\varepsilon_2 \equiv \frac{3}{2} - \frac{t^2}{d^2}$; $\varkappa_\pm \equiv \frac{\lvert t\rvert}{\lvert h\rvert}\ \frac{\lvert t\rvert}{\lambda}$	(12)
$\gg 1$	$Ch\left(\lambda_\circ^{-1}\int_0^r \cos^\nu\frac{\pi}{2}\frac{x}{a}\right) Ch\frac{r}{h}\cos^\nu\frac{\pi}{2}\frac{r}{a}\cos^{-\frac{3}{2}\frac{\pi}{2}\frac{r}{a}} e^{-\varepsilon/\cos^\vartheta\frac{\pi}{2}\frac{r}{a}}$	$Q\, e^{-\varepsilon}$ (by definition)	(18)
	$A\frac{H}{H_a}\frac{n}{n_a}\left(\frac{T}{T_a}\right)^{-3/2} e^{-E/T}$	$dJ_\circ/d\left(\frac{E}{T_a}\right) \langle\sigma v\rangle_a H_a n_a a\, d\Omega$	
$\frac{E}{T_a} \sim 1$	$e^{\left(\gamma^{-1}+\frac{E}{T_a}\tau^{-1}\right)(r-a)-E/T_a}$	$\frac{2}{\sqrt{\pi}}\left(\frac{E}{T_a}\right)^{1/2}\frac{dE}{T_a}\frac{e^{-E/T_a}}{a\left\lvert\gamma^{-1}+\frac{E}{T_a}\tau^{-1}\right\rvert}$	(14)

Definition of profile parameters: t, h, d see Eq. (8)
γ, τ, see Eq. (13)
ϑ, ν, see Eq. (16)

Table 4

$$F \equiv T_o / T_{\phi n}; \quad T_{\phi n}^{-1} = E_n^{-1} \ln \frac{J_o(E_n)}{J_o(2E_n)}$$

(= correction factor rescaled to the "slope temperature between energies E_n and 2 E_n) for $h^{-1} = .7 \lambda_o^{-1}$

density profile: flat

T_o keV	ϑ	$E_n / T_{\phi n}$	a/λ_o 1	2	4	10
		1.0	.79	1.17	3.7	-
		2.0	.85	.89	1.53	5.4
.3	1.5	4.0	.92	.92	1.00	1.97
		8.0	.96	.97	.95	1.19
		1.0	.79	.91	2.9	-
		2.0	.87	.86	1.16	3.8
.7	1.5	4.0	.93	.91	.94	1.54
		8.0	.97	.97	.95	1.07

Table 4 (continued)

density profile: cosine

T_o keV	ϑ	$E_n / T_{\phi n}$	a/λ_o 1	2	4	10
		1.0	.77	.96	2.1	-
		2.0	.87	.91	1.38	3.55
.3	1.5	4.0	.93	.92	1.03	1.87
		8.0	.96	.96	.97	1.23
		1.0	.77	.83	1.58	-
		2.0	.88	.88	1.09	2.6
.7	1.5	4.0	.94	.92	.96	1.5
		8.0	.97	.96	.96	1.1